Available online at www.sciencedirect.com

SciVerse ScienceDirect

Ceramics International 38 (2012) 6163–6169

CERAMICS INTERNATIONAL

www.elsevier.com/locate/ceramint

Silicon carbide particle reinforced mullite composite foams

S. Akpinar[a,*], I.M. Kusoglu[b], O. Ertugrul[c], K. Onel[c]

[a]Afyon Kocatepe University, Department of Material Science and Engineering, Afyonkarahisar, Turkey
[b]Dokuz Eylul University, Torbalı Vocational School, Izmir, Turkey
[c]Dokuz Eylul University, Department of Metallurgical and Materials Engineering, Izmir, Turkey

Received 26 March 2012; received in revised form 19 April 2012; accepted 20 April 2012
Available online 6 May 2012

Abstract

Silicon carbide particle reinforced mullite composite foams were produced by the polymer replica method using alumina and kaolin to form in situ mullite matrix. Up to 20 wt.% silicon carbide particles (SiCp) were added to aqueous ceramic slurry to explore its effect on the rheological behaviour of ceramic slurries and also properties of as sintered products. By means of solid loading optimisation and sintering enhancement by silicon carbide, mullite based ceramic composite foams of higher strength were obtained. The strength of the as sintered foams was found to depend greatly on the phase composition, relative density of the structures and the amount of SiCp addition. By studying the effect of the additive concentration, on the mechanical properties of the ceramic matrix, it is found that the optimal silicon carbide addition is 20 wt.%.

© 2012 Elsevier Ltd and Techna Group S.r.l. All rights reserved.

Keywords: D. Ceramic foam; Mullite; Rheology; SiC

1. Introduction

Ceramic foams are porous materials that consist of a three dimensional array of polyhedral cells, with large voids of the size ranging from 10 μm to several millimetres. The actual cell shape of the foam however is affected by several factors, including the fabrication process [1]. Depending on their morphology the foams can be used as filters of molten metals and exhaust gases, radiant burners, catalyst supports, biomedical devices, kiln furniture, bioreactors, fibre-free thermal management components, supports for space mirrors, components in solid oxide fuel cells, lightweight sandwich structures, heat sinks and heat exchangers [1,2].

The most common route for producing reticulated porous ceramics is the replication method [3]. This method is based on the impregnation of a polymer sponge with a ceramic suspension or precursor solution in order to produce a macro porous ceramic having the same morphology as the original porous material. In the polymer replica approach, a highly porous polymeric sponge is initially soaked into a ceramic suspension until internal pores are filled in with ceramic material. The impregnated sponge is then passed through rollers to remove the excess suspension and enable the formation of a thin ceramic coating over the struts of the original cellular structure of polymer sponge. At this stage, the slurry has to be sufficiently fluid to be partially removed under the shearing conditions applied by the rollers, but the remaining ceramic wet coating should be viscous enough to avoid dripping. Therefore, ceramic suspensions exhibiting shear-thinning behaviour are needed to efficiently coat the polymeric template. The ceramic coated polymeric template is subsequently dried and pyrolysed through careful heating between 300 and 800 °C. Heating rates usually lower than 1 °C/min are required in this step to allow the gradual decomposition and diffusion of the polymeric material, avoiding the buildup of pressure within the coated struts. After removal of the polymeric template, the ceramic coating is finally densified by sintering at temperatures ranging from 1100 to 1700 °C depending on the material [4].

However, these materials have relatively low strength, since only thin webs of the ceramic structure remain after the pyrolysis of the template, a process which also frequently generates longitudinal strut cracks [5]. The major processing problem arises from difficulty in coating

---

*Corresponding author. Tel.: +90 272 2281423; fax: +90 272 2281422.
E-mail address: akpinar@aku.edu.tr (S. Akpinar).

0272-8842/$36.00 © 2012 Elsevier Ltd and Techna Group S.r.l. All rights reserved.
http://dx.doi.org/10.1016/j.ceramint.2012.04.067

the sharp edges of the struts. After coating, the thickness of slurry in these regions is much lower than in other areas. The flaws that lead to cracks in struts are probably regions where the cast ceramic coating is very thin over the protruding triangular edges of the struts [6]. Therefore, several methods have been proposed to improve the mechanical properties of reticulated porous ceramics, by either increasing the strength of the struts or reducing the defects associated with the sharp apices of the triangular voids within the struts. For example, the addition of fibres and whiskers to the ceramic structure was found to effectively strengthen the ceramic struts. Also, a recoating process was used to eliminate the large flaws in the struts, such as cracks and triangular voids [5]. Clearly an approach to overcome the cracking problem would be to increase the coating thickness relative to the polymer strut radius, or to reduce the severity of thin areas at the strut edges, where the coating is most susceptible to cracking. A second coating of slurry may be applied to fill in any flaws or thin areas in the first coating. This second coating will be more difficult to apply since the foam cannot be compressed because this would fracture the original coating. Also, recoating may produce higher density materials that may be less desirable for the intended application of the foam [6]. Therefore, the coating thickness of green ceramic scaffold can be increased by using slurry having favourable rheological behaviour facilitated by high solid loading instead of recoating process.

Mullite is the only intermediate stable compound in the SiO_2–$A1_2O_3$ system. Its properties such as high melting point ($>1800\,^{\circ}C$), low thermal expansion ($4.5-5.6\times 10^{-6}\,^{\circ}C^{-1}$), good thermal shock fracture resistance, low true density (3.16–3.22 g/cm^3), high creep resistence and good chemical stability can be compared with the properties of Si_3N_4 and SiC in terms of being a candidate for high temperature structural materials applications [7]. Using low cost raw materials such as kaolinite, kaolinite–alumina and sillimanite minerals, it is possible to produce high purity mullite [8]. The sintering of mullite powders require high temperature and long thermal treatment as mullite particles have poor solid state sinterability due to the low interdiffusion rates of Si^{4+} and Al^{3+} within the mullite lattice [8,9]. On the other hand, mass production of porous filters requires pressureless, low-temperature, and short-time sintering steps. For this reason it is necessary to use an appropriate sintering aid in amount so as to decrease the high activation energy for ion diffusion through the mullite lattice. There are many possible additives, which act as sintering aids and grain growth inhibitors. Among these additives, magnesia (MgO) is the most consumed and effective one in obtaining mullite products with high density using relatively low temperatures and shorter sintering periods. Addition of 1 wt% magnesia improves the densification of mullite powder, giving rise to more compact and well developed microstructures [9]. However the application of mullite has been limited because it has low fracture stress and fracture toughness at room temperature, as compared with nonoxide ceramics such as silicon carbide and silicon nitride. For this reason, research on mullite matrix composites has been conducted to improve both fracture stress and fracture toughness. For example, SiC whisker, β-Si_3N_4 and both SiC whisker and ZrO_2 particle reinforced mullite composites have been reported. The use of whiskers, however, is expensive and has difficulty in processing. In contrast, research on ceramic particle reinforced mullite has been rare and its characteristics are not well understood [10]. A suitable way to prepare mullite ceramics with low dimensional changes is the reaction bonding process, using SiC and α-Al_2O_3 as the starting materials, because the sintering-induced shrinkage is compensated by the SiC oxidation induced volume expansion. At high temperatures, the surface of SiC is oxidised to SiO_2 and then the latter with high reactivity reacts with α-Al_2O_3 to produce mullite. SiC particles are bonded by in situ formed mullite, to obtain mullite bonded SiC ceramics [11].

Effects of SiC addition on the structure and properties of reticulated porous mullite ceramics were studied in our previous work, where a second coating (recoating) by spray technique was applied to improve the mechanical properties of porous mullite ceramics [12]. The present work aims to improve the mechanical properties of the foam by obtaining a thicker single coating by using ceramic slurry of optimum reological properties prepared by means of SiC addition and appropriate solid loading.

2. Experimental work

As porous template starting material, a commercial polyurethane sponge having a cell size of 20 ppi (pores per inch) was used to produce mullite foams. In order to quantify thermal behaviour of polyurethane sponge, simultaneous thermal analyses (differential thermal analysis, DTA and thermo-gravimetric analysis, TG) were performed in air at a heating rate of 10 °C/min (DTG-60 H, Shimadzu Corporation). Particle size distribution analyses of raw materials were done by using Malvern Mastersizer-2000 model analyser. Specific surface area analyses were done by using Quantachrome Nova-2200e model BET equipment. The results are given in Table 1 for particle size distribution and specific surface area.

As starting raw materials 41.6 wt.% α-Al_2O_3 and 51.4 wt.% kaolin were used for the formation of mullite phase. Gibbsite and MgO were added as sintering aids to the mixtures in amounts of 5 and 1 wt.% respectively. A total amount of 1 wt.% Carboxymethyl cellulose (CMC) and bentonite were added to the mixtures for thickening and improving the rheological behaviour of the slurry. The major additive to the mixtures was SiC powder where the added amounts were 0, 5, 10, 15 and 20 wt.%. The prepared powder mixtures are encoded as M_0, M_5, M_{10}, M_{15} and M_{20} where, ‘M’ stands for mullite while ‘0, 5, 10, 15 and 20’ stand for wt.% SiC. The chemical compositions of the raw materials are listed in Table 2. The compositions

Table 1
Particle sizes and specific surface areas of raw materials.

Raw materials	Particle size (μm)			Spesific surface area (m^2/g)
	$d_{0.9}$	**$d_{0.5}$**	**$d_{0.1}$**	
Gibbsite	–	–	–	300
Magnesia	120.40	23.79	2.70	1.98
Kaolin	31.17	9.82	3.19	11.80
Alumina	32.78	6.51	2.24	1.43
SiC	75.32	40.41	20.21	0.17

Table 2
Chemical compositions of raw materials.

Composition (wt %)	**Kaolin**	**Alumina**	**Magnesia**	**Gibbsite**	**Bentonite**
SiO_2	48.34	0.02	0.97	0.01	67.52
Al_2O_3	36.83	98.98	0.33	64.65	12.78
Fe_2O_3	0.70	0.02	0.48	0.02	0.83
TiO_2	0.04	0.08	0.00	0.00	0.06
CaO	0.08	0.00	1.46	0.00	1.96
K_2O	1.86	0.00	0.00	0.00	2.39
Na_2O	0.04	0.42	0.00	0.30	0.79
MgO	0.28	0.00	96.47	0.00	1.40
Ignition loss	12.14	0.41	0.29	35.02	12.27

Table 3
Compositions of powder mixtures.

Composition (wt.%)	**M_0**	**M_5**	**M_{10}**	**M_{15}**	**M_{20}**
Kaolin	51.40	48.83	46.26	43. 69	41.12
Alumina	41.60	39.52	37.44	35.36	33.28
Magnesia	1.00	0.95	0.90	0.85	0.80
Bentonite	0.75	0.71	0.68	0.64	0.60
Gibbsite	5.00	4.75	4.50	4.25	4.00
CMC	0.25	0.24	0.22	0.21	0.20
SiC	0	5	10	15	20

of powder mixtures are given in Table 3. The slurries of M_5, M_{10}, M_{15} and M_{20} were prepared so that each solution had solid loading levels given in Table 3, and 0.8 wt.% commercial deflocculant Dolapix CE-64 (Zschimmer and Schwarz, Germany) was added to achieve a good dispersion of ceramic particles in aqueous solution.

The slurry was prepared in distilled water. At first, distilled water was mixed with CMC and Dolapix CE-64 by stirring for 5 min. Then, kaolin and bentonite were added into solution and mixed for 30 min. The other ceramic powders were subsequently added to the solution and ground for 15 min using alumina balls.

A rheological study has been carried out in order to optimise the processing of the porous mullite foams by using a rotational stress-controlled rheometer (Bohlin-CVO model rheometer). The measurements were performed at constant temperature (20 °C) using a cone and plate configuration. A pre-shearing was performed at high shear rate ($1000\ s^{-1}$) for 1 min before the measurement was followed by an equilibrium time for 30 s to transmit the same rheological history to all tested suspensions. Sweep measurements were then conducted in the shear rates ranging from about $0.1–1000\ s^{-1}$.

The polyurethane sponge pieces were firstly immersed in the slurry. Then the impregnated sponge pieces were passed through a set of rotating rollers to remove excess slurry. The distance between the preset rollers was 20% of the sponge thickness. Ceramic coated sponge pieces were dried at room temperature for 24 h. Dried samples were heated to 600 °C at a heating rate of 1 °C/min in order to burn out the sponge material according to the results of DTA-TG analysis. Subsequently, the samples were heated to 1600 °C at a rate of 5 °C/min and sintered in air for 4 h. The linear shrinkage of samples during the course of sintering was determined using the following equation below

$$\text{Shrinkage} = \frac{lg - l\text{p}}{lg} \times 100\%$$

where lg is the height of green sample and lp is the height of fired product. The height was measured by sliding gauge. Bulk density of the sintered foam samples (ρb) was calculated from dimensional measurements and mass of the sintered samples. Solid density (ρs) of the samples was determined using Micromeritics Accu pyc II 1340 model gas (helium) pycnometer on crushed sintered foams consisted of the single struts and the broken cell walls.

The microstructures were observed by scanning electron microscopy (SEM) (Model JSM-6060 JEOL, Japan). Phase analysis of the sintered samples was conducted by standard powder X-ray diffractometer (RIGAKU, Japan). Compressive strength (σ_c) of the sintered samples having dimensions of 50 mm × 50 mm × 10 mm was measured using a Shimadzu (Japan) universal testing machine fitted with compression plates, at a cross-head speed of 0.5 mm/min. Five samples were tested for each type of material while determining properties of the foams.

3. Results and discussion

As seen in Fig. 1, the decomposition of polyurethane sponge takes place in three stages in air. The first stage, which starts at approximately 220 °C and continues up to 350 °C showing a small endothermic signal at about 300 °C which is probably the beginning of decomposition. In the second stage (350–450 °C), a higher intensity exothermic signal is observed at about 400 °C, where weight loss is almost complete due to burn out of the carbon produced by decomposition of the polymer sponge and the generation of gas during the polymer oxidation. There is no significant weight loss in the third stage (450–600 °C), so the major fraction of polymer is burnt out between 220 and 600 °C. These observations are comparable with those of Dressler et.al. [13]. The decomposition step is very important to prevent the ceramic structure from destruction, due to the high pressure of the generated gas,

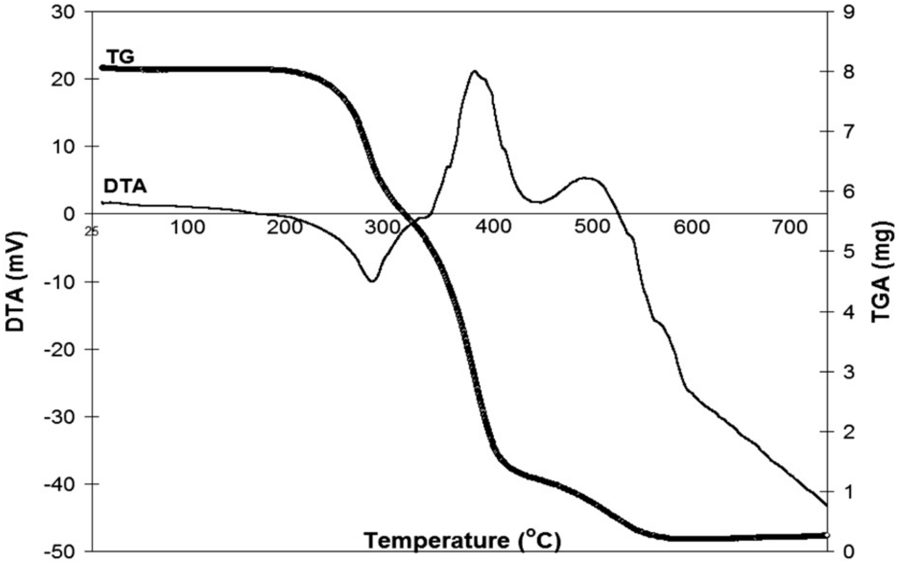

Fig. 1. Differential thermal (DTA) and thermal gravity (TG) curves of the green polyurethane sponge at a heating rate of 10 °C/min.

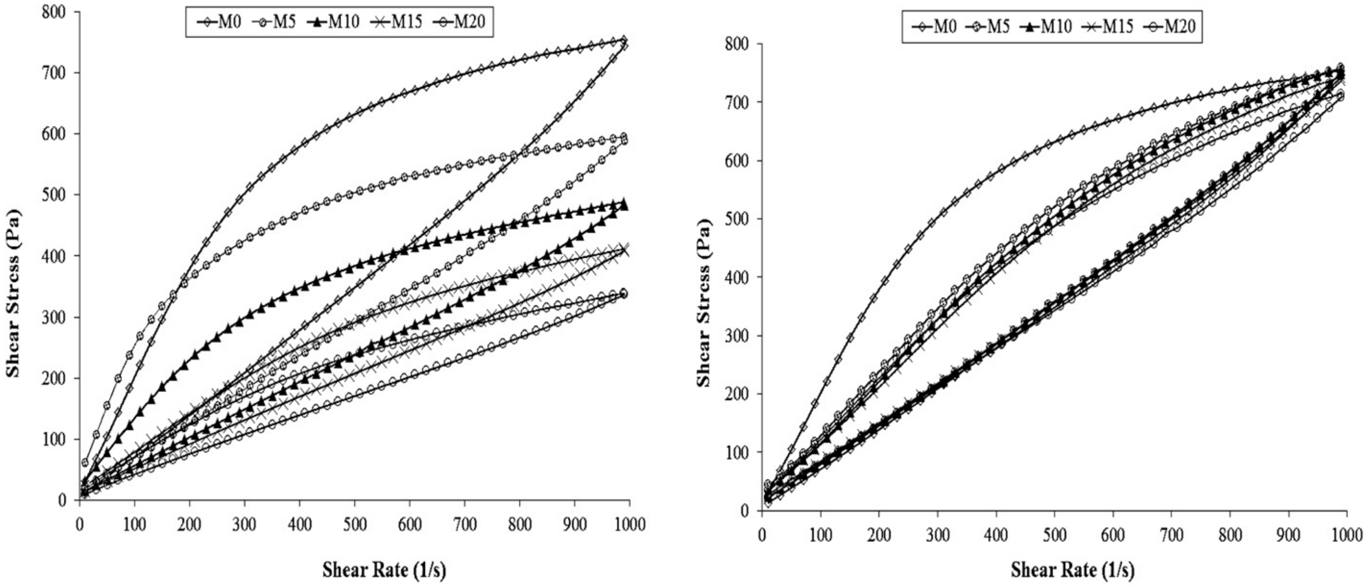

I. State

II. State

Fig. 2. Effect of SiC content on the reological properties of mullite solutions.

which detoriates mechanical properties of ceramic foam. For that reason, a slow heating rate of 1 °C/min was used up to 600 °C for damage free removal of the organics from the ceramic foam bodies.

Fig. 2 shows the effect of SiC content on the reological properties of mullite solutions. In order to achieve a ceramic coating of acceptable characteristics on a polyurethane foam scaffold, the slurry should have the appropriate thixotropic or shear-thinning behaviour [14]. The thixotropic behaviour of slurry is characterised generally by measuring the thixotropic loop between the ascending and descending parts of the flow curve. In descending part of the curve, the shear stress is lower due to the breaking down the bond chain through the suspension and deflocculating phenomenon. This means when polymeric sponge is impregnated with ceramic slurry, suspension is fluid enough to enter, fill and uniformly coat sponge web and subsequently regain enough viscosity under static conditions to remain on sponge [15].

The flow curves in Fig. 2 labelled as State I show the effect of SiC content on the thixotropic behaviour of slurries with the same level of solid loading (with 67% solid content), as shown in Table 4. The distance between ascending and descending parts and shear stress values decrease with increasing SiC content in State I curves. The two samples which include 15 and 20% SiC have nearly

Table 4
Solid contents of solutions used to coat the sponge.

Code	Solid content of solutions (%)	
	State I	*State II*
M_0	67.00	67.00
M_5	67.00	69.86
M_{10}	67.00	70.10
M_{15}	67.00	70.70
M_{20}	67.00	71.10

lost their thixotropic behaviour and exhibit almost Newtonian flow behaviour.

In order to obtain the same favourable thixotropic behaviour of slurries of different amount of SiC additions, the solid contents of the slurries have been optimised. In Table 4 the optimum solid loading ratios of SiC containing slurries are given. As the added amount of SiC is increased the slurries of slightly higher solid contents are needed in order to obtain acceptable and similar thixotropic behaviour to the slurry without SiC addition. In Fig. 2 State II shows the flow curves of SiC containing slurries with optimised solid contents.

The polymer sponges were firstly dipped in suspensions having thixotropic behaviours given as state II, then passed through the rollers. Then as coated sponges rotated 90° and passed again through the rollers. After keeping for few minutes at static condition the coated sponges passed through the rollers again to have fractional and anisotropic forming. Here, percentage of compression changes the volume of slurry squeezed out of the foam on the first pass. Additional passes remove less slurry but often redistribute the retained slurry, improving large-scale uniformity. However, filled cells and cell faces often remain at or near the surfaces of the sample that are perpendicular to the roller surfaces during compression. These surfaces often retain filled cells even after repeated compression. This probably occurs because much of the slurry that is squeezed out exits through these perpendicular surfaces, but there is not enough force to expel the last of the material from the foam structure. Therefore, it was helpful to rotate the samples between passes so that the faces which were in contact with the roller surfaces during the first pass were perpendicular during the second pass. This also helps to improve the large-scale uniformity [6].

After driying, sponge burn out and sintering, the samples have been characterised and mechanical properties have been determined. The properties of as sintered foams are given in Table 5.

It is seen in Table 5 that shrinkage values in sintered samples without SiC addition are approximately 17.5% and decreases to 5% with increasing SiC content. This is mainly due to the decrease in kaolin content used for mullite phase synthesis and volume expansion effect of SiC upon oxidation. The bulk density of the sample without SiC addition is 0.48 g/cm^3 and it decreases to 0.41 g/cm^3 with the addition of 10 wt.% SiC then increases to 0.44 g/cm^3 when 20 wt.% SiC is added. True densities of the samples are between 2.62 and 2.89 g/cm^3. In the literature, the density of mullite phase is stated to be 3.16 g/cm^3 [16]. It is obvious that the theoretical density values are not reached in the produced samples, and the true density values decrease with increasing SiC content. The decrease in true density values is attributed to the decrease in corundum content while SiC content is increased, as SiC having lower density (3.20 g/cm^3) than corundum phase (3.95 g/cm^3).

Table 5
Properties of the foams.

Sample	Shrinkage (%)	ρ_b (g/cm^3)	σ_t (g/cm^3)	σ_r (g/cm^3)	σ_c (MPa)
M0	17.52	0.48	2.89	0.16	0.50 ± 0.11
M5	12.50	0.42	2.83	0.15	0.42 ± 0.08
M10	9.01	0.41	2.74	0.15	0.63 ± 0.09
M15	5.77	0.43	2.67	0.16	0.71 ± 0.05
M20	5.18	0.44	2.62	0.17	1.11 ± 0.23

The XRD patterns of sintered samples and as received SiC powder are given in Fig. 3. The phase composition of the sample without SiC (M_0) consists of mullite and corundum. With 5 wt.% SiC addition (M_5) intensity of corundum peaks decreased and some of them disseapered. Mullite phase and some SiC peaks with low intensity has been observed in the specimens with 10% SiC addition (M_{10}). Phase compositions of M_{15} and M_{20} samples are similar to that of M_{10} with higher SiC intensities. It is indicated that in the specimen M_5 the added SiC is oxidised and has contributed to mullite phase formation. In the specimen M_{10} some unoxidised SiC is left producing a low intensity peak in the pattern in the products containing 15 and 20 wt.% SiC higher amounts of unoxidised SiC phase is determined. The role of silicon carbide in the mullization is mainly due to its oxidation which provides glassy phase of SiO_2 to activate α-Al_2O_3. Here, active α-Al_2O_3 is more effective for the formation of secondary mullite by addition of SiC.

It is seen in Table 5 that compressive strength values of the products are in the range 0.42–1.11 MPa. Maximum value in strength is reached by the samples containing 20 wt.% SiC. As seen in Table 5, the mean compressive strength of the 5% SiC reinforced mullite foams was 0.42 MPa, lower than that of the samples without silicon carbide addition. This is mainly due to the fact that corundum has higher compressive strength than mullite [17], and SiC addition of up to 10 wt.% has contributed to mullite phase formation in the foam structure. The strengthening mechanism of silicon carbide addition in the M_{10}, M_{15} and M_{20} series mainly lies on the composite structure occurred by its dispersion in the aluminium-silicate solid solution between mullite grains and its higher compressive strength than mullite.

The most significant property describing the behaviour of porous ceramics is the relative density (ρ_r), which is the ratio of the sample bulk density (ρ_b) to the solid density

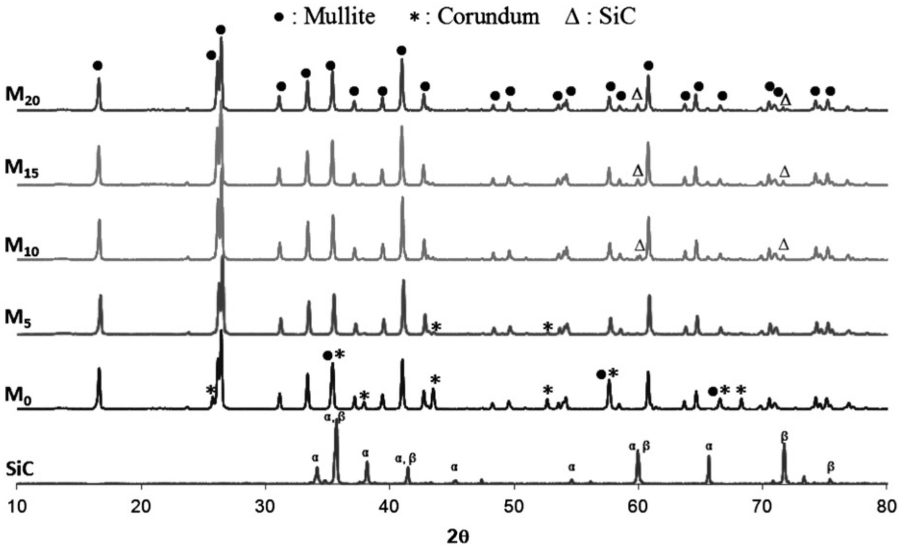

Fig. 3. XRD patterns of the sintered foam samples.

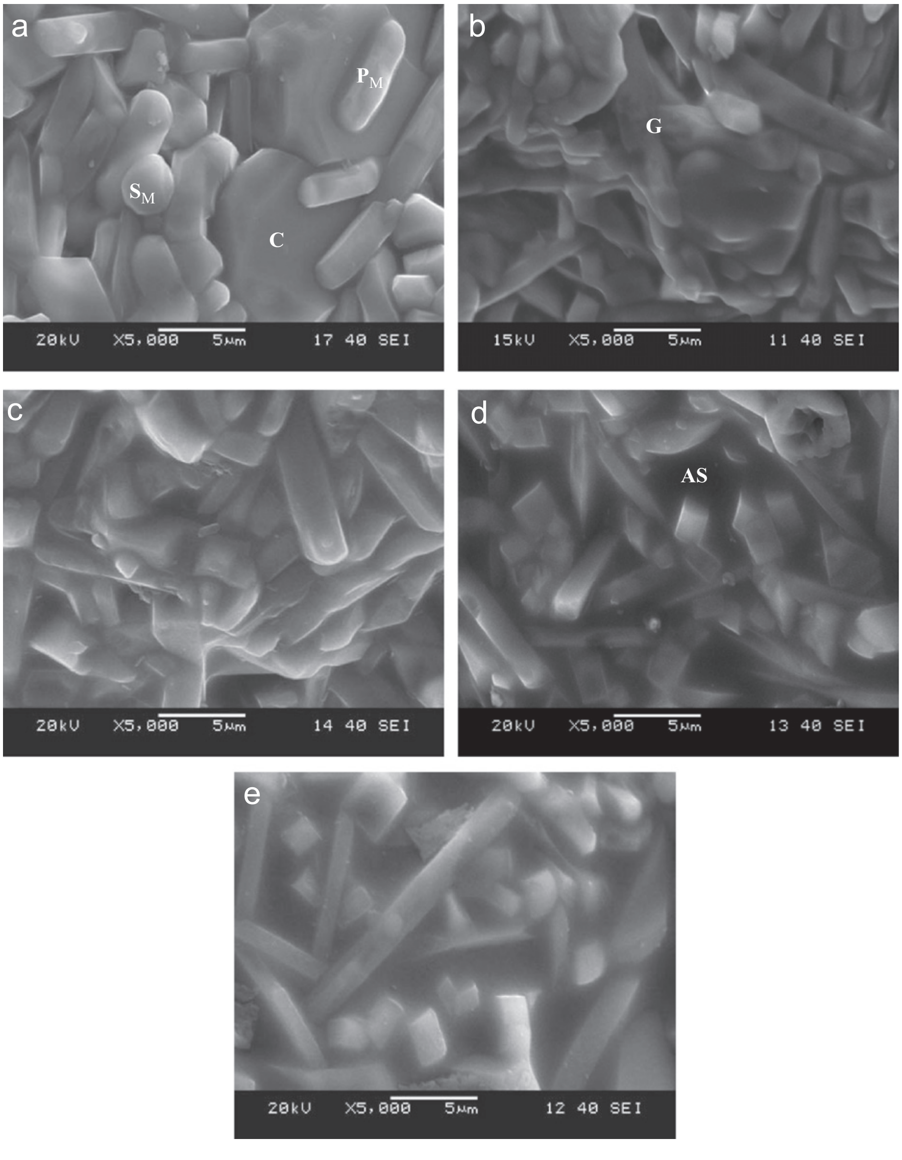

Fig. 4. SEM pictures of the samples with (a) 0, (b) 5, (c) 10, (d) 15 and (e) 20 wt. % SiC content. (P_M: primer mullite, S_M: seconder mullite, C: corundum, AS: alumina-silicate, G: glassy phase).

(ρ_s). There are micromechanical models that relate the solid properties and the foam properties such as the relative density, the cell size and the geometry to mechanical behaviour. The most applicable method to predict the mechanical behaviour of cellular ceramics is the model that has been published by Gibson and Ashby. They used a simple unit cell and described the failure in structure by the failure of cell struts. Maiti et al. applied the Gibson and Ashby (GA) model to describe the compressive strength of brittle porous materials. The crushing strength of the cellular body (σ_{fs}) via the strut strength and relative density is been expressed by the following equation:[15].

$$\sigma_{cr} = C\sigma_{fs}(\rho/\rho_s)^{3/2} \tag{1}$$

According to this equation, the samples with 5 wt.% SiC addition have the lowest mean compressive strength (0.42 MPa) as they possess the lowest relative density (0.15) as given in Table 5. Experimental results confirm this prediction; the samples with 20 wt.% SiC have higher relative density values (0.17) and some SiC reinforcement, as expected, exhibit higher compressive strength (1.11 MPa).

The SEM pictures of the sintered samples are given in Fig. 4. EDX analysis has been carried out in some matrix and grain zones and evaluated in relation to macro and microstructures. The microstructure of the sample without SiC (M_0) consists of primary and secondary mullite grains, unreacted corundum grains and porosity. With the addition of 5 wt.% SiC (M_5), porosity level is decreased and glassy phase is formed by the oxidation of SiC particles which is solidified around corundum grains without complete mullitization. With 10 wt.% SiC addition (M_{10}), silicon carbide containing aluminosilicate phase thought to be existent in between the mullite grains so there is no corundum grains and porosity observed. With 15 and 20 wt.% SiC addition (M_{15} and M_{20}), mullite grains are well dispersed within increased SiC containing aluminasilicate phase.

4. Conclusions

The main conclusions can be deduced from the results presented in this work are that the addition of silicon carbide particle to mullite mixtures affects the flow curves of the slurries, the shrinkage after firing, the phases that form during sintering and the properties of the products.

With SiC addition to mullite slurries, the viscosity decreases, and the rheological behaviour is altered. Favourable rheological behaviour can be established by increasing the solid loadings to adequate levels in the silicon carbide containing slurries.

The shrinkage of a sample without silicon carbide addition is approximately 17.5%. With the addition of SiC the shrinkage decreases gradually to about 5%. The decrease in shrinkage is attributed to decrease in kaolin content in the base composition by the addition of SiC and volume expansion effect of glassy SiO_2 phase during the oxidation of SiC.

The sintered samples with up to 10 wt.% particulate silicon carbide (SiCp) consist of mullite and corundum phases. The samples with 10, 15 and 20 wt.% SiC addition (M_{10}, M_{15} and M_{20}) consist of Mullite phase and SiC particles in increasing amounts with increasing SiC addition.

The strength of the sintered samples is affected by the phases present in the structure. The samples which contain mullite and silicon carbide (M_{20}) exhibit higher strength than the samples containing mullite and corundum (M_0).

References

[1] L.J. Gibson, M.F. Ashby, Cellular solids: structure and properties, 2nd ed., Cambridge University Press, Cambridge, 1997.

[2] P. Colombo, Ceramic Foams: fabrication, properties, and applications, Key Engineering Materials 206-213 (2002) 1913–1918.

[3] J. Luyten, I. Thijs, W. Vandermeulen, S. Mullens, B. Wallaeys, R. Mortelmans, Strong ceramic foams from polyurethane templates, Advances in Applied Ceramics 104 (2005) 1.

[4] A.R. Studart, U.T. Gonzenbach, E. Tervoort, L.J. Gauckler, Processing routes to macroporous ceramics: a review, Journal of the American Ceramic Society 89 (6) (2006) 1771–1789.

[5] I.K. Jun, Y.H. Koh, J.H. Song, S.H. Lee, H.E. Kim, Improved compressive strength of reticulated porous zirconia using carbon coated polymeric sponge as novel template, Material Letters 60 (20) (2006) 2507–2510.

[6] D. Brown, D.J. Green, Investigation of strut crack formation in open cell alumina ceramics, Journal of the American Ceramic Society 77 (6) (1994) 1467–1472.

[7] L. Montanaro, J.M. Tulliani, C. Perrot, A. Negro, Sintering of industrial mullites, Journal of the European Ceramic Society 11 (1997) 1715–1723.

[8] V. Viswabaskaran, F.D. Gnanama, M. Balasubramanian, Effect of MgO, Y_2O_3 and boehmite additives on the sintering behaviour of mullite formed from kaolinite-reactive alumina, Journal of Materials Processing Technology 142 (2003) 275–281.

[9] E. Roncari, C. Galassi, C. Bassarello, Mullite suspensions for reticulate ceramic preparation, Journal of the American Ceramic Society **83** (12) (2000) 2993–2998.

[10] S. Sato, M.C. Chu, Y. Kobayashi, K. Ando, Strengthening of mullite by dispersion of carbide ceramics particles, Japanese Society of Mechanical Engineering 39 (2) (1996) 259–265.

[11] S. Ding, S. Zhu, Y.P. Zeng, D. Jiang, Fabrication of mullite-bonded porous silicon carbide ceramics by in situ reaction bonding, Journal of European Ceramic Society 27 (2007) 2095–2102.

[12] S. Akpınar, I.A. Altun, K. Onel, Effects of SiC addition on the structure and properties of reticulated porous mullite ceramics, Journal of European Ceramic Society 30 (13) (2010) 2727–2734.

[13] M. Dressler, S. Reinsch, R. Schadrack, S. Benemann, Burnout behavior of ceramic coated open cell polyurethane sponges, Journal of European Ceramic Society 29 (2009) 3333–3339.

[14] X. Yao, S. Tan, Z. Huang, D. Jiang, Effect of recoating slurry viscosity on the properties of reticulated porous silicon carbide ceramics, Ceramics International 32 (2006) 137–142.

[15] Z. Negahdari, M. Solati, Fabrication of Reticulated Porous Mullite Refractories as a Molten Metal Foam Filter, UNITECR'05, In: Proceedings of the Unified International Technical Conference on Refractories, 2005.

[16] D.W. Richerson, Modern ceramic engineering: properties, processing and use in design, 2nd Ed., Marcel Dekker, New York, 1992.

[17] J.F. Shackelford, W. Alexander, CRC materials science and engineering handbook, CRC Press, Boca Raton, Fl, 2001.